X-ray scattering from periodic arrays of quantum dots

2008 J. Phys.: Condens. Matter 20 454215

(http://iopscience.iop.org/0953-8984/20/45/454215)

J. Phys.: Condens. Matter **20** (2008) 454215 (6pp) doi:10.1088/0953-8984/20/45/454215

X-ray scattering from periodic arrays of quantum dots

V Holý[1], J Stangl[2], R T Lechner[2] and G Springholz[2]

[1] Department of Condensed Matter Physics, Faculty of Mathematics and Physics, Charles University, Ke Karlovu 5, 121 16 Praha, Czech Republic
[2] Institute of Semiconductor Physics, Kepler University, Altenbergerstrasse 69, A-4040 Linz, Austria

E-mail: holy@physics.muni.cz

Received 6 May 2008, in final form 2 July 2008
Published 23 October 2008
Online at stacks.iop.org/JPhysCM/20/454215

Abstract
Three-dimensional periodic arrays of self-organized quantum dots in semiconductor multilayers are investigated by high-resolution x-ray scattering. We demonstrate that the statistical parameters of the dot array can be determined directly from the scattering data without performing a numerical simulation of the scattered intensity.

1. Introduction

High-resolution x-ray scattering is frequently used for the investigation of the structure of semiconductor quantum dots (see the review in [1], for instance).

The aim of an x-ray scattering experiment is to determine (i) the positions of the dots in the sample, (ii) the mean size and shape of quantum dots and (iii) the strain field in and around the dots. Combining the x-ray data with elasticity simulations it is possible to estimate local chemical composition in quantum dots.

For the goals (i) and (ii) one can use the chemical contrast between the dot lattice and the crystal matrix, i.e. the contrast in the electron density averaged over the unit cell. The chemical contrast can be investigated in a small-angle scattering experiment, in which the scattering vector $\mathbf{Q} = \mathbf{K}_f - \mathbf{K}_i$ ($\mathbf{K}_{i,f}$ are the wavevectors of the primary and scattered beams, respectively) is much smaller than the size of the first Brillouin zone. For the investigation of strains, the sensitivity of the **h**th Fourier component of the electron density to tiny atomic displacements is used, where **h** is a reciprocal-lattice vector (diffraction vector). Then, the scattering vector is chosen close to the diffraction vector (x-ray diffraction).

Since a scattering experiment yields a reciprocal-space distribution of the scattered intensity, its interpretation is not straightforward. Usually, the measured intensity map is compared with the results of simulations, based on a suitable structural model, which includes also a numerical simulation of elastic strains in and around the dots. A direct determination of the dot structure from the diffraction data can be possible only using a phase-retrieval algorithm [2]. In this work we demonstrate that the statistical parameters of the dot positions (task (i) in the list above) can be determined *directly* from the measured diffraction data without any *a priori* chosen structural model.

2. Elements of x-ray scattering theory

Since a single dot is much smaller than the extinction length of x-rays in the lattice (several microns), the scattering process in the dot volume can be assumed fully kinematical. However, if the dots are embedded in a thick crystal matrix, multiple scattering effects in the matrix play a role and the scattering in the matrix is dynamical. A theoretical description of dynamical x-ray scattering from a crystal with an array of quantum dots is rather complicated and usually one uses an experimental arrangement, in which the deviation from the kinematical approximation comprises only the effects of absorption and refraction at the sample surface. These two effects can be included in the simulation replacing the scattering vector **Q** by the corrected scattering vector $\mathbf{Q}_T = \mathbf{k}_f - \mathbf{k}_i$, where $\mathbf{k}_{i,f}$ are the complex wavevectors of the transmitted beams in the substrate, corresponding to the vacuum waves with the wavevectors $\mathbf{K}_{i,f}$. In the following, we omit the subscript $_T$ for simplicity.

In a standard scattering experiment, the number of irradiated dots is rather large. In addition, the primary x-ray beam is usually much broader than its coherence width, so that the irradiated sample contains many coherently irradiated volumes. Then the measured intensity is an incoherent

superposition of the contributions of many volumes with different dot positions. If the number of coherently irradiated volumes is very large, the scattered intensity can be considered averaged over the statistical ensemble of all dot configurations

$$I_{\mathbf{g}}(\mathbf{Q}) = \left\langle E_{\mathbf{g}}(\mathbf{Q}) E_{\mathbf{g}}^{*}(\mathbf{Q}) \right\rangle, \qquad \mathbf{g} = 0, \mathbf{h}. \tag{1}$$

In the case of small-angle scattering, this averaging can be performed directly; for diffraction only an approximative numerical averaging can be carried out. In both geometries, the scattered intensity can be expressed in a similar way [1, 3]:

$$I_{\mathbf{g}}(\mathbf{Q}) \sim N_{\mathrm{D}}[\langle |F_{\mathbf{g}}(\mathbf{Q})|^2 \rangle - |\langle F_{\mathbf{g}}(\mathbf{Q}) \rangle|^2] + |\langle F_{\mathbf{g}}(\mathbf{Q}) \rangle|^2 C(\mathbf{Q}), \quad \mathbf{g} = 0, \mathbf{h}. \tag{2}$$

Here we have denoted N_{D} the total number of dots in the coherently irradiated volume:

$$F_{\mathbf{g}}(\mathbf{Q}) = \int_V \mathrm{d}^3\mathbf{r} \mathrm{e}^{-\mathrm{i}(\mathbf{Q}-\mathbf{g})\cdot\mathbf{r}} \times \left[\chi_{\mathbf{g}}^{\mathrm{matrix}} \left(\mathrm{e}^{-\mathrm{i}\mathbf{g}\cdot\mathbf{u}(\mathbf{r})} - 1\right) + \Delta\chi_{\mathbf{g}} \Omega(\mathbf{r}) \mathrm{e}^{-\mathrm{i}\mathbf{g}\cdot\mathbf{u}(\mathbf{r})}\right] \tag{3}$$

is the structure factor of a single dot, $\Omega(\mathbf{r})$ is the shape function of a single dot (unity in the dot volume and zero outside it), $\chi_{\mathbf{g}}^{\mathrm{matrix}}$ is the $\mathbf{g}$th polarizability coefficient in the matrix, $\Delta\chi_{\mathbf{g}}$ is the difference of $\chi_{\mathbf{g}}$ in the dot and in the matrix, and $\mathbf{u}(\mathbf{r})$ is the displacement field caused by a single dot. For small-angle scattering ($\mathbf{g} = 0$), the structural factor equals $\Delta\chi_0 \Omega^{\mathrm{FT}}(\mathbf{Q})$, where $^{\mathrm{FT}}$ denotes the Fourier transformation, so that the averages $\langle |F_0|^2 \rangle$ and $|\langle F_0 \rangle|^2$ can easily be calculated. For diffraction, this averaging is a difficult numerical task, since it must include a complicated numerical simulation of the displacement field for all dot sizes included in the averaging.

In equation (3) we have denoted

$$C(\mathbf{Q}) = \left\langle \sum_{\mathbf{R},\mathbf{R}'} \mathrm{e}^{-\mathrm{i}(\mathbf{Q}\cdot\mathbf{R} - \mathbf{Q}^*\cdot\mathbf{R}')} \right\rangle \tag{4}$$

as the correlation function of the dot positions; in this expression $\mathbf{R}$, $\mathbf{R}'$ are the random dot position vectors. The form of the correlation function depends on the type of the statistical arrangement of the dots in the sample volume.

The first term in equation (2) is a slowly varying function of $\mathbf{Q}$ and usually gives rise to an almost non-structured background. If the dot positions are at least partially correlated, the correlation function $C(\mathbf{Q})$ in the second term exhibits sharp maxima and, as we show in the next section, their forms can be used for a direct determination of the statistical parameters of the dot positions, without performing a complicated numerical evaluation of the averages of the structure factor.

3. Three-dimensional arrangements of self-organized quantum dots

In this section, we present a simple phenomenological model describing the positions of self-organized quantum dots in a periodic multilayer. The multilayer consists of N identical vertical periods of thickness D, each period contains a dot layer of material A and a spacer layer and its material B is usually the same as the material of the buffer layer or substrate underneath.

We assume that lateral position $\mathbf{X}_{jn}$ of the jth dot at the interface n depends only on the lateral positions of the dots at the preceding interface $n-1$. The nature of the correlation in the dot positions at different interfaces is not discussed here; as we demonstrated in a series of works [4–6], this correlation is caused by the strains originating from buried dots and propagated through the spacer layer. In [7] another mechanism is proposed leading to the correlation in the dot positions, namely the influence of the buried dots on the morphology of the growing surface, which affects the two-dimensional diffusion of adatoms and consequently the probability of nucleation of the dots at the growing surface.

Independently of the correlation mechanism, the sequence of lateral position vectors $\mathbf{X}_{j0}, \mathbf{X}_{j1}, \ldots, \mathbf{X}_{jN}$ represents a simple Markov chain and for its description we use standard statistical methods. The correlation function of the dot position is

$$C(\mathbf{Q}) = \sum_{j,j'} \sum_{n,n'} \mathrm{e}^{-\mathrm{i}(Q_z Z_n - Q_z^* Z_{n'})} \left\langle \mathrm{e}^{-\mathrm{i}\mathbf{Q}_\parallel \cdot (\mathbf{X}_{jn} - \mathbf{X}_{j'n'})} \right\rangle, \tag{5}$$

where $\mathbf{R}_{jn} = (\mathbf{X}_{jn}, Z_n)$ is the three-dimensional position vector of the dot (j, n), while its non-random vertical coordinate $Z_n = nD$ is a multiple of the multilayer period D. In the following, we denote $n = 0$ as the surface of the substrate or of a buffer layer under the dot multilayer. In the case of perfectly arranged dots, the dots will create a three-dimensional lattice with the basis vectors $\mathbf{a}_{1,2,3}$. We choose these vectors so that the vectors $\mathbf{a}_{1,2}$ lie in the plane parallel to the sample surface and the vertical component a_{3z} of the third vector $\mathbf{a}_3$ equals the multilayer period D.

In the following we denote $\mathbf{U}_{jn} = \mathbf{X}_{jn} - \mathbf{X}_{jn-1} + \mathbf{a}_{3\parallel}$ as the lateral displacement of the dot (j, n) with respect to its ideal lateral position $\mathbf{X}_{jn-1} + \mathbf{a}_{3\parallel}$ with respect to the preceding dot $(j, n-1)$. Since we assume that the lateral positions of the dots at different interfaces n, n' are correlated only for $n = n' \pm 1$, the deviations $\mathbf{U}_{jn}$ and $\mathbf{U}_{j'n'}$ are not correlated, i.e.

$$\left\langle \mathbf{U}_{jn} \cdot \mathbf{U}_{j'n'} \right\rangle = \sigma^2 \delta_{jj'} \delta_{nn'} \tag{6}$$

holds, where σ is the root-mean-square (rms) deviation of the displacements $\mathbf{U}$.

The correlation function $C(\mathbf{Q})$ depends on the correlation function $C_0(\mathbf{Q}_\parallel)$ of the positions of the dots at the interface $n = 0$. A direct calculation yields

$$C(\mathbf{Q}) = M^2 S_1(|\psi|^2) + [G_0(\mathbf{Q}_\parallel) - M^2] S_1(|\psi\xi|^2) + 2\mathrm{Re}\{M^2 S_2(\psi\xi, \psi^*/\xi) + [G_0(\mathbf{Q}_\parallel) - M^2] \times S_2(\psi\xi, \psi^*\xi^*)\}, \tag{7}$$

where

$$\psi(\mathbf{Q}) = \mathrm{e}^{-\mathrm{i}\mathbf{Q}\cdot\mathbf{a}_3}$$

and

$$\xi(\mathbf{Q}_\parallel) = \left\langle \mathrm{e}^{-\mathrm{i}\mathbf{Q}_\parallel \cdot \mathbf{U}} \right\rangle$$

is the characteristic function of the probability distribution of the random displacement $\mathbf{U}$. If we assume a normal distribution with the rms deviation σ, we obtain

$$\xi(\mathbf{Q}_\parallel) = \mathrm{e}^{-\sigma^2 |\mathbf{Q}_\parallel|^2/2}.$$

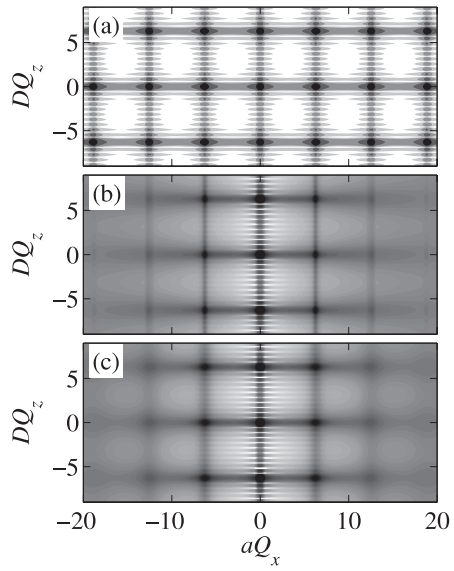

Figure 1. The correlation function $C(Q_x, 0, Q_z)$ of an ideally periodic three-dimensional dot arrangement (a). The panels (b) and (c) show the correlation function calculated using the LRO and SRO models, respectively. Notice that the lateral FWHMs ΔQ_x of the satellites do not depend on Q_x within LRO (panel (b)), while they increase with Q_x in the SRO model (c). Within both models, the vertical FWHMs ΔQ_z increase with increasing $|Q_x|$.

In equation (4) we denoted

$$S_1(a) = \sum_{n=0}^{N} a^n = \frac{a^{N+1} - 1}{a - 1}$$

and

$$S_2(a, b) = \sum_{n=1}^{N} \sum_{m=0}^{n-1} a^n b^m = \frac{1}{b-1}\left[\frac{(ab)^{N+1} - ab}{ab - 1} - \frac{a^{N+1} - a}{a - 1}\right].$$

The correlation function $G_0(\mathbf{Q}_\parallel)$ describes the position of the 0th dot array at the substrate surface. The choice of this function depends on the sample structure; if the 0th dot array is deposited at a flat substrate (or buffer) surface, the dot positions usually obey a two-dimensional short-range-order (SRO) model [8]. If the substrate surface is lithographically patterned before the dot growth, the ideal dot positions are defined by the pattern and a two-dimensional long-range-order (LRO) model is more appropriate [9].

The two-dimensional SRO correlation function can be approximated by a direct product of two one-dimensional SRO correlation functions:

$$G_0(\mathbf{Q}_\parallel) = M^2 \prod_{p=1,2}\left[1 + 2\mathrm{Re}\left(\frac{\omega_p}{1 - \omega_p}\right)\right]. \qquad (8)$$

Here we have denoted M^2 the number of dots at an interface assumed very large:

$$\omega_p(\mathbf{Q}_\parallel) = \left\langle \mathrm{e}^{-\mathrm{i}\mathbf{Q}_\parallel \cdot \mathbf{b}_p} \right\rangle, \qquad p = 1, 2$$

and $\mathbf{b}_{1,2}$ are the random vectors connecting the neighboring dots in the $\mathbf{a}_{1,2}$ directions, respectively. Calculating the averages $\omega_{1,2}$ we consider that $\langle \mathbf{b}_{1,2} \rangle = \mathbf{a}_{1,2}$ and we introduce the rms deviation σ_0 of the lengths of the random vectors $\mathbf{b}_{1,2}$.

The correlation function in equation (8) describes an ideal two-dimensional SRO model and this function diverges for $\mathbf{Q}_\parallel \cdot \mathbf{a}_{1,2} = 0$. In order to remove this non-physical divergence we consider a finite number M of the dots along the $\mathbf{a}_1$ or $\mathbf{a}_2$ axes. Then, M^2 denotes the number of dots in a domain, in which the SRO model can be applied; usually the size of this domain corresponds to the coherence width of the primary x-ray beam. If the distance of two dots is larger than this coherence width, they are irradiated incoherently and the waves scattered from these dots cannot interfere. Using a finite value of M, the correlation function has the form

$$G_0(\mathbf{Q}_\parallel) = \prod_{p=1,2}\left[M + 2\mathrm{Re}\left(\frac{\omega_p}{1 - \omega_p}(M - 1) - \frac{\omega_p^2}{(1 - \omega_p)^2}(1 - \omega_p^{M-1})\right)\right]. \qquad (9)$$

In a practical calculation, we usually assume that the number M is random, too, and we average this correlation function over M. This averaging removes rapid non-physical oscillations in the correlation function, the period of which is inversely proportional to M. For this averaging, the binomial probability distribution of M can be used among others, with a given mean $\langle M \rangle$ and a suitably chosen rms dispersion.

In the case of an LRO arrangement of the dots at the substrate interface the correlation function $G_0(\mathbf{Q}_\parallel)$ must be described in another way. We assume that the dot $(j, 0)$ deviates from its ideal position $j_1\mathbf{a}_1 + j_2\mathbf{a}_2$ by a random displacement $\mathbf{U}_{j0}$. If the displacements of two different dots are not correlated then

$$\left\langle \mathbf{U}_{j0}, \mathbf{U}_{j'0} \right\rangle = \sigma_0^2 \delta_{jj'}$$

holds, where σ_0 is the rms deviation of the displacement. A direct calculation yields the following expression for the correlation function:

$$G_0(\mathbf{Q}_\parallel) = M^2\left[1 - |\omega|^2\right] + |\omega|^2 G_0^{\mathrm{id}}(\mathbf{Q}), \qquad (10)$$

where

$$\omega(\mathbf{Q}_\parallel) = \left\langle \mathrm{e}^{-\mathrm{i}\mathbf{Q}_\parallel \cdot \mathbf{U}_{j0}} \right\rangle = \mathrm{e}^{-\sigma_0^2 |\mathbf{Q}_\parallel|^2/2}$$

and

$$G_0^{\mathrm{id}}(\mathbf{Q}_\parallel) = \sum_{j_1=1}^{M} \sum_{j_2=1}^{M} \mathrm{e}^{-\mathrm{i}\mathbf{Q}_\parallel \cdot (j_1\mathbf{a}_1 + j_2\mathbf{a}_2)}$$

is the correlation function of a perfectly ordered two-dimensional dot array. Similarly to the SRO model, the parameter M^2 denotes the number of dots in one coherent domain and usually the correlation function G_0 is averaged over M in order to remove non-physical oscillations.

In figures 1 and 2 we present the correlation function $C(Q_x, 0, Q_z)$ calculated for a dot multilayer assuming a tetragonal arrangement of dots ($\mathbf{a}_1 = (a, 0, 0), \mathbf{a}_2 = (a, 0, 0), \mathbf{a}_3 = (0, 0, D)$) and $N = 10$ multilayer periods.

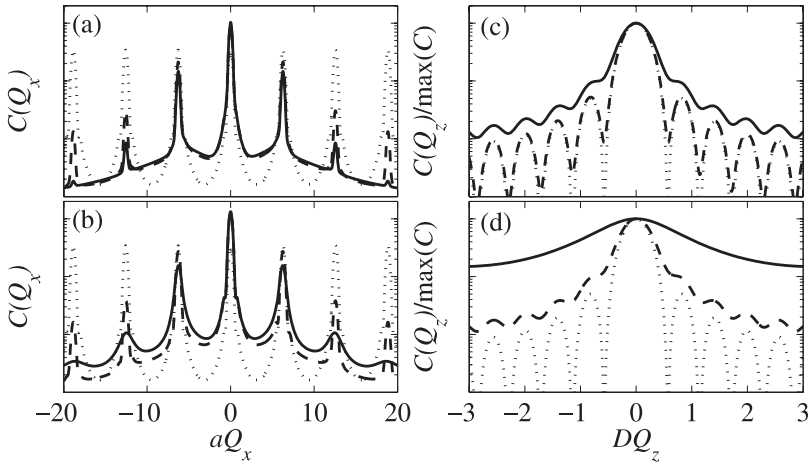

Figure 2. Panels (a) and (b) show the correlation function $C(Q_x, 0, 0)$ calculated in the LRO (a) and SRO (b) models for $\sigma_0 = 0$ (dotted), $0.01a$ (dashed) and $0.1a$ (full lines). In (c) and (d), the functions $C(Q_x = \text{const}, 0, Q_z)$ are plotted for the first lateral maximum ($Q_x = 2\pi/a$) (c) and the second maximum ($Q_x = 4\pi/a$) (d). The curves in (c) and (d) were calculated for $\sigma = 0$ (dotted), $0.05D$ (dashed) and $0.1D$ (full lines). After normalization to their maximum values, the curves in (c) and (d) are identical for LRO and SRO models.

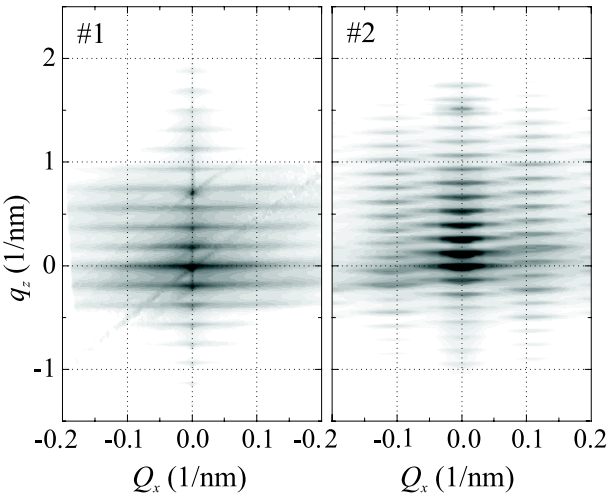

Figure 3. Reciprocal-space maps of the PbSe/PbEuTe multilayers (samples #1 and #2) measured in symmetric coplanar diffraction 111. The step of the intensity contours is $10^{0.2}$.

From figure 1 it is obvious that the correlation function exhibits satellite maxima in the points of the lattice reciprocal to the averaged dot lattice. From the dependence of the full widths at half-maximum (FWHMs) $\Delta Q_{x,z}$ of these maxima on $Q_{x,z}$ we can determine the type of correlation function and the parameters σ, σ_0, and the averaged number $\langle M \rangle$. In the following, this number will be denoted as M, for simplicity.

Due to the ideal vertical periodicity of the multilayer, the two-dimensional distribution of the C values is ideally periodical along Q_z with the period $2\pi/D$. In the case of the LRO arrangement of the dots at the substrate interface, the lateral FWHM $\Delta Q_x = 2\pi/(Ma)$ is constant and it is inversely proportional to the size of the coherent domain. This behavior can be seen in figure 1(b), where the width of the lateral satellites along Q_x is constant and independent of Q_x. For the SRO arrangement, the lateral FWHM increases with increasing Q_x. The satellites in figure 1(c) in the Q_x direction become broader indeed for larger $|Q_x|$. In the limit of very large coherent domain ($M \to \infty$), $\Delta Q_x \to (Q_x\sigma_0)^2/a$ holds and the lateral FWHM of the satellites is proportional to the square of the satellite order.

In the LRO and SRO models, the vertical shapes of the satellites determined by the function $C(Q_x = \text{const}, Q_z)$ are similar. If we normalize the functions $C(Q_x = \text{const}, Q_z)$ to their maxima, both LRO and SRO models yield the same profiles $C(Q_x = \text{const}, Q_z)$. This is obvious from figures 2(c) and (d), where we have plotted the vertical profiles $C(Q_x = \text{const}, Q_z)$ of the satellites for the first- (figure 2(c)) and second-order (figure 2(d)) lateral satellites. The profiles are normalized to their maxima and identical functions were obtained from both models. Therefore, the FWHM ΔQ_z is the same for SRO and LRO arrangements and it depends on σ and on the number N of the multilayer periods. In the limit $N \to \infty$, $\Delta Q_z \to (Q_x\sigma)^2/D$ holds, similarly to the ΔQ_x in the SRO model.

From this numerical analysis a simple recipe follows how to determine the parameters of the dot ordering from the measured intensity map. From the dependence of the horizontal FWHM ΔQ_x of the satellites on Q_x we can distinguish between two ordering models introduced above: if the FWHM does not depend on Q_x, the LRO model is applicable, and from the FWHM we determine the average number M of the dots in the coherent domain. If the FWHM ΔQ_x grows with increasing $|Q_x|$, the SRO model is appropriate and from the fit of the experimental dependence $\Delta Q_x(Q_x)$ we determine the rms deviation σ_0 and the average number M of the dots in the coherent domain. The dependence of the vertical FWHM ΔQ_z on Q_x is the same for both models; the fit of this dependence to the theory yields the rms deviation σ.

From the analysis above it follows that the FWHMs ΔQ_x and ΔQ_z depend only on the lateral coordinate Q_x (figures 1(a)–(c) are perfectly periodic along Q_z). A possible

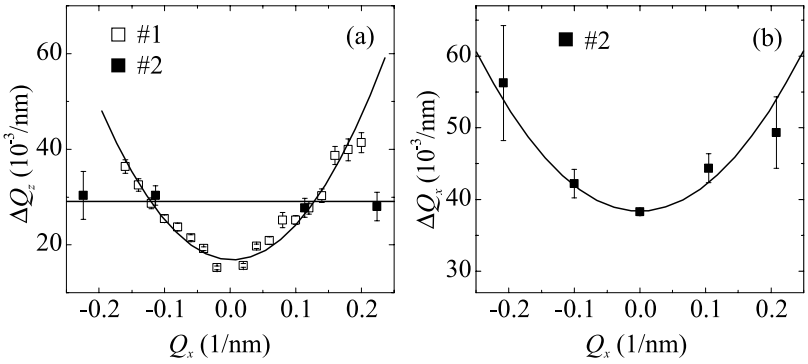

Figure 4. The Q_x dependence of the vertical (a) and lateral (b) FWHMs of the intensity satellites of the PbSe/PbEuTe multilayers (points) and their theoretical fits (lines).

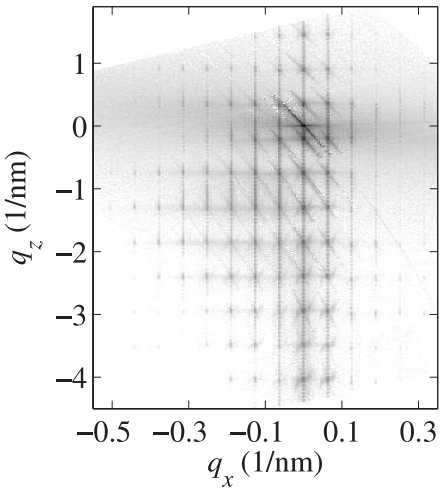

Figure 5. Reciprocal-space map of a Ge/Si multilayer measured in the coplanar asymmetric 224 diffraction.

dependence of the experimental FWHMs on Q_z could be ascribed to the Q_z dependence of the resolution function of the experimental set-up or to a non-periodicity of the multilayer along z.

4. Experimental examples

In this section we present two experimental examples demonstrating the application of the above theory. As the first example, figure 3 shows the intensity maps of PbSe/PbEuTe multilayers deposited by molecular beam epitaxy (MBE) on a PbTe(111) buffer layer on a BaF_2 substrate. The samples differ in the thicknesses of the PbEuTe spacer layers—in sample #1 the smaller thickness of 36 nm gives rise to a strong vertical ordering of the PbSe layers, while in the case of thicker spacer layer (47 nm, sample #2) the PbSe dots create a rhombohedral lattice (see [6] for more details). The measurements have been carried out at ESRF Grenoble, in symmetric coplanar diffraction 111, using the wavelength 1.54 Å. In figure 3 we denoted $q_z = Q_z - h_z$ and h_z is the vertical coordinate of the diffraction vector $\mathbf{h} = 111$.

The maxima in the maps correspond to the local maxima of the correlation function $C(\mathbf{Q})$. The map of sample #1 exhibits only horizontal sheets indicating that the dots are correlated mainly vertically. The maxima in the map of sample #2 create a well-developed three-dimensional lattice; from their positions it follows that the lattice of the dots is rhombohedral. Figure 4 shows the dependence of the FWHMs $\Delta Q_{x,z}$ of the maxima on Q_x. In sample #1 the ordering of the dots at the 0th interface is very weak and σ_0 is very large. Therefore, no distinct lateral satellites are present in its intensity map in figure 3 and we could determine only the dependence $\Delta Q_z(Q_x)$. The parabolic dependence $\Delta Q_z(Q_x)$ confirms the validity of the ordering model formulated above; from the fit to the theory the value $\sigma = (5 \pm 1)$ nm follows.

For sample #2 the rms deviation σ is very small, since the vertical FWHM ΔQ_z does not depend on Q_x; we estimate $\sigma < 0.2$ nm. The dependence $\Delta Q_x(Q_x)$ is nearly parabolic, so that the SRO model for the ordering of the dots at the 0th g interface is applicable. From the fit to theory we determined $\sigma_0 = (6 \pm 1)$ nm and $M = 7 \pm 2$. Therefore, in sample #2, the dot positions at subsequent interfaces are almost ideally correlated; the disorder of the dots stems from the dots at the buffer surface.

In the second example we investigate the positions of Ge dots in an Si/Ge multilayer deposited by MBE on an Si(001) surface, on which a periodic square array of pits have been lithographically created (see [10] for details). An asymmetric coplanar reciprocal-space map measured in diffraction 224 is plotted in figure 5, where we have denoted $q_{x,z} = Q_{x,z} - h_{x,z}$ the reciprocal-space vector relative to the reciprocal-lattice point $\mathbf{h} = 224$. The measurement has been carried out at ESRF Grenoble, using the wavelength 1.5 Å. Sharp satellite maxima indicate that the dots are very well correlated both horizontally and vertically. A detailed analysis of the FWHMs (figure 6) demonstrates that the LRO model (equations (7) and (10)) is valid—in contrast to the previous example the lateral satellite FWHMs ΔQ_x do not depend on Q_x. From the fit of the vertical FWHMs ΔQ_z we obtain $\sigma = (3.5 \pm 0.5)$ nm, while the lateral FWHMs yield $M = 6 \pm 1$. The resulting size $Ma = 600$ nm of the coherent domain is comparable with the coherence width of the primary radiation.

5. Summary

We demonstrated that from the dependence of the widths of the intensity satellites on their position (Q_x, Q_z) in reciprocal

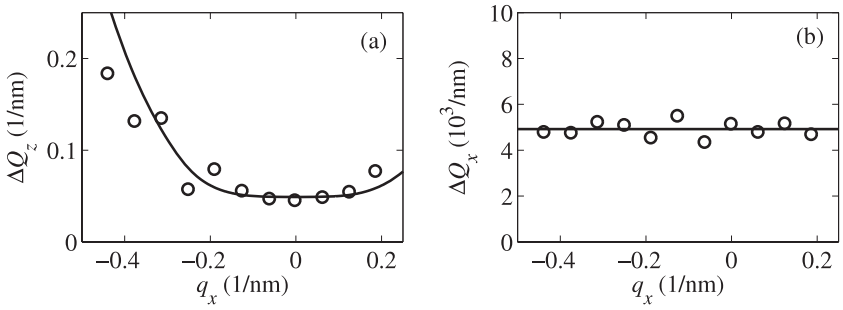

Figure 6. The q_x dependence of the vertical (a) and lateral (b) FWHMs of the intensity satellites of the Ge/Si multilayer and their theoretical fits (lines).

space it is possible to determine the type of correlation of the dot positions and to estimate the rms deviations of the dot distances. This procedure is direct and does not require any numerical simulation of elastic strains and diffracted intensities.

Two examples shown in this paper, namely PbSe dots in PbSe/PbEuTe multilayers and Ge dots in SiGe multilayers deposited on a pre-patterned Si substrate, represent two different cases of the self-organization. In the former case, the dots at the first interface on a PbTe buffer are distributed according to a short-range-order model, while in the latter case a long-range order of the dot positions on the substrate surface is induced by the pre-patterning. The dot positions at subsequent interfaces are correlated to the dots underneath, and for their positions the short-range-order model can be used in both systems.

Acknowledgment

This work was supported by the research program MSM0021620834 that is financed by the Ministry of Education of the Czech Republic.

References

[1] Stangl J, Holý V and Bauer G 2004 *Rev. Mod. Phys.* **76** 725
[2] Pfeifer M A, Williams G J, Vartanyants I A, Harder R and Robinson I K 2006 *Nature* **442** 63
[3] Revenant C, Leroy F, Lazzari R, Renaud G and Henry C R 2004 *Phys. Rev.* B **69** 035411
[4] Springholz G, Holý V, Pinczolits M and Bauer G 1998 *Science* **282** 734
[5] Holý V, Springholz G, Pinczolits M and Bauer G 1999 *Phys. Rev. Lett.* **83** 356
[6] Springholz G, Pinczolits M, Mayer P, Holý V, Bauer G, Kang H H and Salamanca-Riba L 2000 *Phys. Rev. Lett.* **84** 4469
[7] Buljan M, Desnica U V, Dražić G, Ivanda M, Radić N, Dubček P, Salamon K, Bernsdorff S and Holý V 2008 *Nat. Mater.* submitted
[8] Pukite P R, Lent C S and Cohen P I 1985 *Surf. Sci.* **161** 39
[9] Wollschläger M and Larsson M 1998 *Phys. Rev.* B **57** 14937
[10] Grützmacher D, Fromherz T, Dais C, Stangl J, Müller E, Ekinci Y, Solak H H, Sigg H, Lechner R T, Wintersberger E, Birner S, Holý V and Bauer G 2007 *Nano Lett.* **7** 3150